Limit Condition for Fiber-Reinforced Granular Soils

RADOSLAW L. MICHALOWSKI AND AIGEN ZHAO

Approximate methods for analysis and synthesis of earth structures using such reinforcement as geotextiles or geogrids have been used successfully for more than two decades. Soil reinforcement with short fibers and continuous synthetic filaments has been tried in the past decade. Although the latter has been used with success in construction practice, no techniques for design with such materials exist. This is mainly the result of poor understanding of the fiber-matrix (filament-matrix) interaction and, consequently, lack of appropriate models capable of describing the stress-strain behavior and failure of such composites. An attempt at describing the failure criterion of fiber-reinforced sand is presented. The properties of the constituents are approximated by their standard characteristics: the Mohr-Coulomb failure function for the granular matrix and the Tresca criterion for fibers. The failure of the composite is considered to be because of the collapse of the matrix associated with intact fibers or with fibers failing in slip or the tension mode. An energy-based homogenization technique is used. Results of some preliminary laboratory experiments are also presented. Application of the derived failure criterion is shown in an example of a slope limit load problem.

Although considerable progress in design methods with traditional reinforcement (geotextiles, geogrids, etc.) has been made in the past decade, no techniques for design with fiber-reinforced or continuous filament-reinforced soil exist. This is predominantly because of poor understanding of the behavior of such composites, even though successful applications are known (*1*).

This paper focuses on a failure criterion for fiber-reinforced soils using a plasticity-based technique. A limit surface is found in the macroscopic stress space, which describes stress states associated with failure of a fibrous composite with a granular matrix.

Elastic and elastoplastic behavior of composite materials has been described using various methods of homogenization (averaging), ranging from self-consistent schemes (*2–4*) to the finite element approach (*5*). An excellent survey of techniques used for analysis of composite materials was presented in a work by Hashin (*6*); since then, significant interest in fiber composites has been maintained.

Little attention has been paid to composites with granular or low-cementitious matrices. Failure criteria of such materials must be known to evaluate the stability of structures such as reinforced soil slopes. Existing literature includes only a handful of papers with attempts at describing theoretically the behavior of reinforced soil and, particularly, fiber-reinforced or continuous filament-reinforced granular composites (*7–12*). This paper presents a continuation of previous efforts toward constructing a consistent model for predicting failure of fiber-reinforced soils.

Radoslaw L. Michalowski, Department of Civil Engineering, The Johns Hopkins University, Baltimore, Md. 21218. Aigen Zhao, Tenax Corp., 4800 East Monument St., Baltimore, Md. 21205.

Experimental results from tests on specimens of fiber-reinforced soils are available (*13–17*). Development of a strength criterion based on considering behavior of fibers intersecting a strain localization zone (shear band) dominates among the theoretical efforts triggered by experimental observations. Strain localization should be avoided in mathematical homogenization schemes or when testing for material properties, because the boundary displacements are no longer representative of the strain of the entire material within a specimen. This does not contradict the usefulness of the direct shear test where parameters for a well-defined model are tested. A common interpretation of results from tests on fiber-reinforced samples is a piecewise linear failure condition, with the first range (at low confining stresses) relating to fiber slip and the second one associated with fiber yielding. Whereas such two clearly different ranges of behavior can be conjectured intuitively, a sharp transition, often suggested in the literature, appears to be the outcome of a loose interpretation of the test results.

This paper is intended to introduce the concept of homogenization and macroscopic description to fiber-reinforced soils. It presents the preliminary results, theoretical and experimental, but, for brevity, the details of theoretical derivation and experimental techniques are omitted here.

Fundamentals of the homogenization technique used will be presented in the next section, followed by a brief description of the failure criterion for fiber-reinforced soil. Next, some experimental results from triaxial tests on specimens of sand reinforced with steel and polyamide fibers will be presented. The paper is concluded with an example of the application of the derived failure criterion and some final remarks.

MACROSCOPIC LIMIT STRESS

The term "macroscopic stress" is used here to represent the average stress in the composite. Because the failure criterion is of interest, the macroscopic stress at the limit state is investigated. The homogenization technique used here is based on consideration of the energy dissipation during plastic deformation (yielding) of the composite. It is required that the work performed by the macroscopic stress $\bar{\sigma}_{ij}$ during an incipient plastic deformation process of a representative element be equal to the rate of dissipation $\dot{D}(\dot{\epsilon}'_{ij})$ in the constituents (matrix and fibers) of the composite

$$\bar{\sigma}_{ij}\dot{\epsilon}_{ij} = \frac{1}{V}\int_V \dot{D}(\dot{\epsilon}'_{ij})\,dV \tag{1}$$

where

V = volume of a representative element of the composite,
$\dot{\epsilon}_{ij}$ = macroscopic (average) strain rate, and
$\dot{\epsilon}'_{ij}$ = microstrain rate in the composite constituents.

This technique is similar to using limit analysis, except that here the unknown limit load is the average stress in the composite at failure. A concept similar to this was explored earlier in the context of cementitious composites in works by Hashin (*18*) and Shu and Rosen (*19*), and for two-dimensional membranes by McLaughlin and Batterman (*20*).

A linear macroscopic velocity field v_i is assumed here

$$v_i = a_{ij} x_j \tag{2}$$

where x_j is the Cartesian coordinate and a_{ij} is a matrix of coefficients subject to constraints imposed by the dilatancy of the matrix material. We are considering plane-strain deformation; hence Equation 2 becomes

$$\begin{aligned} v_1 &= -\dot{\epsilon}_{11} x_1 - \dot{\epsilon}_{12} x_2 \\ v_2 &= -\dot{\epsilon}_{21} x_1 - \dot{\epsilon}_{22} x_2 \end{aligned} \tag{3}$$

where $\dot{\epsilon}_{ij}$ is the macroscopic strain rate throughout the considered representative element of the composite (compression is taken as positive). Assumption of a linear velocity field has an important consequence: the rate of energy dissipation in yielding fibers depends only on their orientation, not on their particular location in the composite element.

The homogenization technique proposed here is considerably different from that recently suggested in a work by di Prisco and Nova (*10*), who considered a continuous filament reinforcement. In that approach, the macroscopic stress is arrived at by superposition of the stress in the soil matrix and a fictitious filament structure capable of resisting tension only. It is a statics-based approach similar to one used in the mechanics of mixtures. Although it is a very reasonable method for homogenizing the continuous filament composite, the energy-based technique used in this paper is more convenient when slip of fibers needs to be accounted for.

FAILURE CRITERION FOR FIBER-REINFORCED SAND

Failure of the fiber-reinforced composite occurs when the matrix material reaches the yielding state, which may be associated with slip or tensile collapse of fibers. It is assumed here that the matrix material conforms to the Mohr-Coulomb failure condition and the associative flow rule. The strain rate field must then satisfy the dilatancy relation

$$\frac{\dot{\epsilon}_v}{\dot{\epsilon}_1 - \dot{\epsilon}_3} = -\sin \varphi \tag{4}$$

where $\dot{\epsilon}_v = \dot{\epsilon}_{ii}$ is the volumetric strain rate and φ is the internal friction angle of the matrix, which, for the associative flow rule, also indicates the rate of dilation. Under the assumptions made (Mohr-Coulomb criterion, associativity), the rate of energy dissipation during plastic deformation of a noncohesive matrix is zero (*21*). Although a purely granular (noncementitious) matrix is considered here, the effort can be easily extended to cementitious (cohesive) matrices.

The use of the associative (normality) rule for soils has been questioned in the past as it predicts unrealistic rates of dilation (Equation 4). The associative flow rule is not unreasonable; however, this issue deserves more space, and it is not addressed here [the reader will find a useful discussion elsewhere (*22*)].

The amount of fibers is characterized here by their concentration (volume density)

$$\rho = \frac{V_r}{V} \tag{5}$$

where V_r is the volume of the fibers and V is the volume of the entire representative composite element. The yield point of the fibers is σ_0. Fibers contribute to the composite strength only if a tensile force can be mobilized in them. A frictional load transfer mechanism is considered here. An interface shear stress and axial stress in a rigid, perfectly plastic fiber within a uniformly deforming matrix is shown in Figure 1. The maximum tensile stress in fibers (σ_0) can be mobilized only if length l is sufficiently large, otherwise fiber slip occurs. Note that even if the middle part of a fiber is at yield, each of its ends will slip over the distance d (Figure 1).

$$d = \frac{r}{2} \frac{\sigma_0}{\sigma_n \tan \varphi_w} \tag{6}$$

where

σ_n = stress normal to the fiber surface,
φ_w = friction angle of the matrix-fiber interface, and
r = fiber radius.

A uniform distribution of the fiber orientation in three-dimensional space is considered here. The dissipation rate in a single fiber in the deforming matrix depends on the strain in the direction of the fiber. The energy dissipation rate due to fiber tensile collapse was calculated by integrating the dissipation over all the fibers in tension. Contribution of fibers under compression to the strength of the composite is neglected here because of possible buckling and kinking. Because a frictional fiber-matrix interface is assumed in the model, the interface shear stress is dependent on the stress normal to the fibers. Calculations are performed here assuming this stress is equal to the mean of the maximum and minimum stress $p[p = (\bar{\sigma}_1 + \bar{\sigma}_3)/2]$ for all fibers. This assumption leads to a conservative estimate of the energy dissipation rate because the average normal stress on fibers under tension (fibers under compression are excluded in calculations of the dissipation rate) is larger than the mean stress p, and, therefore, the energy dissipation rate due to fiber slip

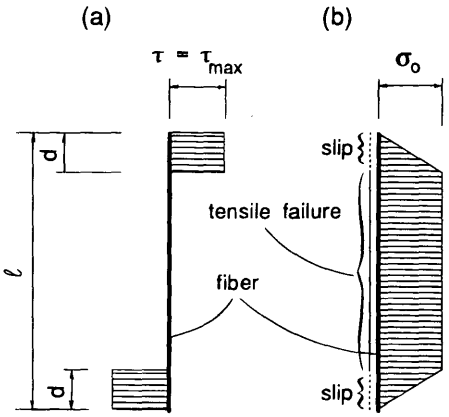

FIGURE 1 Stress distribution on a rigid-plastic fiber in a deforming matrix: (a) interface shear stress; (b) the axial stress.

is underestimated. Consequently, for a uniformly distributed orientation (not uniform orientation) in three-dimensional space, this assumption leads to a conservative estimate of the fiber contribution to strength and is acceptable for such composites. This may not be acceptable for anisotropic patterns of fiber orientation distribution where the mean stress p may be larger than the average normal stress on fibers under tension.

This paper focuses on the concept of macroscopic description itself; the mathematical details of the derivation will not be presented. In short, a plane-strain deformation process of a fictitious composite specimen was considered, and the expression in Equation 1 was used to calculate the macroscopic stress at failure $\bar{\sigma}_{ij}$. It is convenient to represent this failure stress (failure condition) as

$$f = R - F(p) = 0 \quad \text{or} \quad R = F(p) \tag{7}$$

where R is the radius of the limit stress circle, and p is the mean of the extremal principal stresses

$$R = \frac{1}{2}(\bar{\sigma}_1 - \bar{\sigma}_3) = \frac{1}{4}\sqrt{(\bar{\sigma}_x - \bar{\sigma}_y)^2 + 4\tau_{xy}^2}$$
$$p = \frac{1}{2}(\bar{\sigma}_1 + \bar{\sigma}_3) \tag{8}$$

For long fibers where tensile failure can be expected, the failure criterion was found in the form

$$\frac{R}{\rho\sigma_0} = \frac{p}{\rho\sigma_0}\sin\varphi + \frac{1}{3}N\left(1 - \frac{1}{4\rho\eta}\frac{1}{\frac{p}{\rho\sigma_0}\tan\varphi_w}\right) \tag{9}$$

where η is the fiber aspect ratio (r = fiber radius)

$$\eta = \frac{l}{2r} \tag{10}$$

and

$$N = \frac{1}{\pi}\cos\varphi + \left(\frac{1}{2} + \frac{\varphi}{\pi}\right)\sin\varphi \tag{11}$$

When fibers are relatively short ($l \leq 2d$, Figure 1), collapse of the composite is expected to be associated with slip of fibers. This occurs when

$$\eta < \frac{1}{2}\frac{\sigma_0}{p\tan\varphi_w} \tag{12}$$

The failure criterion associated with the slip of fibers takes the form

$$\frac{R}{\rho\sigma_0} = \frac{p}{\rho\sigma_0}\sin\varphi + \frac{1}{3}N\frac{p}{\sigma_0}\eta\tan\varphi_w \tag{13}$$

Note that $\rho\sigma_0$ is used here to normalize the maximum shear stress, and R is independent of the fiber yield stress (σ_0) when pure slip occurs.

The failure criterion is isotropic (uniform distribution of fiber orientation), is independent of the intermediate principal stress (the consequence of the matrix Mohr-Coulomb failure condition), and can be presented conveniently in $\tau_{max} - p$ space ($\tau_{max} = R$). Figure 2 shows the results of calculations for one particular example, where

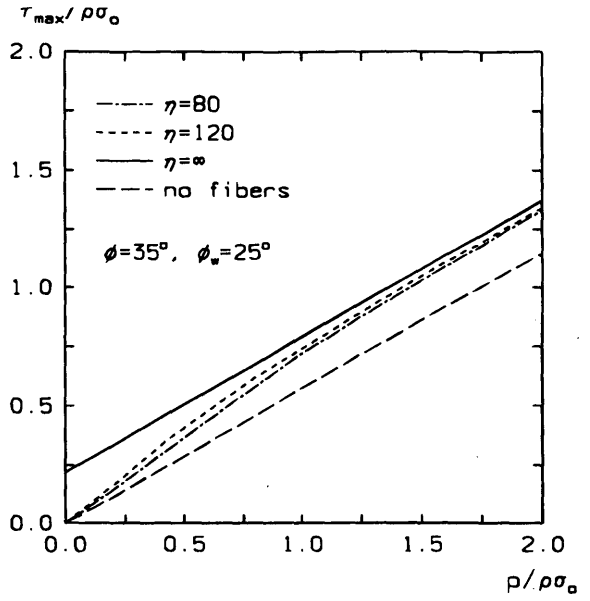

FIGURE 2 Maximum shear stress envelopes for a fiber-reinforced granular material (theoretical result).

constant internal friction angle of the granular matrix $\varphi = 35°$ and angle of fiber-matrix interfacial friction $\varphi_w = 25°$ (this is somewhat higher than what was measured for steel or polyamide). Although the model is sensitive to φ_w, this friction is probably not the single mode of load transfer to the fibers, as will be suggested in the next section. The failure lines are piecewise functions where the range for low p is linear (Equation 13), and it is nonlinear for larger p (Equation 9). Notice that the failure criterion is continuous and smooth (continuous first derivative).

The failure criterion in Equations 9 and 13 is consistent with the constitutive description in the theory of plasticity (irreversible and time-independent behavior of solids) and can be used directly in analytical and numerical techniques for solving boundary value problems in geotechnical engineering. This description is different from the one based on consideration of localized shear during the failure process as proposed elsewhere (*17*). In the latter, the occurrence of strain localization is predetermined, random distribution of fiber orientation is ignored (all fibers are considered perpendicular to the shear band), and the contribution of fibers to the composite strength is assumed a priori to be a linear function of the confining stress. The increase of the shear strength is then expressed as a function of a distortion angle in the shear zone. The second model also introduces an empirical constant, which further contributes to the fact that the two descriptions cannot be reasonably compared.

PRELIMINARY TEST RESULTS

An experimental program is under way to indicate whether the theoretical description derived is a reasonable characterization of the true failure behavior of fiber-reinforced sand. Comprehensive results from the experimental study are unavailable, but some results are presented in Figure 3. Triaxial tests were performed on specimens of fiber-reinforced sand. It should be pointed out that soils do not conform to the Mohr-Coulomb failure criterion precisely; in particular, yielding of soils is sensitive to the intermediate principal

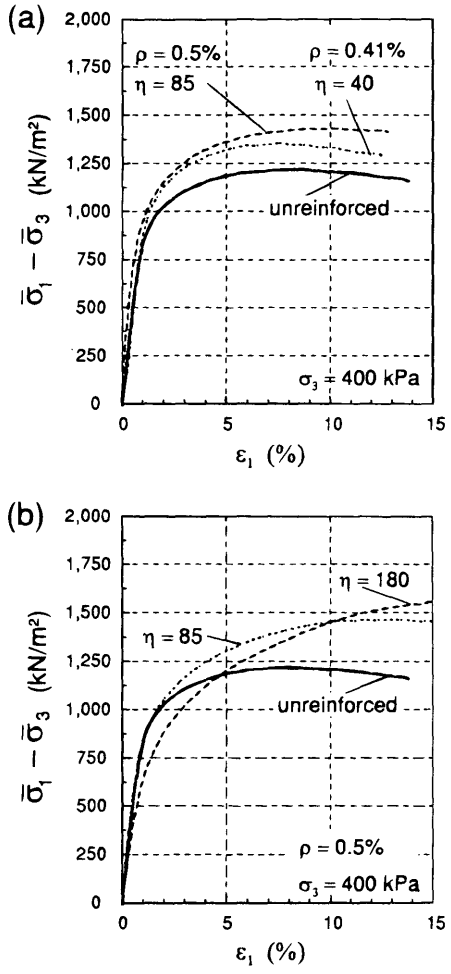

FIGURE 3 Stress-strain curves from drained triaxial tests on fiber-reinforced sand at confining pressure 400 kPa: (a) steel fibers; (b) polyamide fibers.

stress. The results of plane-strain and axisymmetric tests, therefore, can be expected to be different. It is important for consistency that the internal friction of the soil be obtained from the same type of test that is performed for the fiber-reinforced composite. However, because it was decided that the Mohr-Coulomb condition (independent of the intermediate principal stress) be used for the matrix, the results of the theoretical investigation may be expected not to be sensitive on whether it involves plane-strain or axisymmetrical analysis.

A coarse, poorly graded sand was used, with $d_{50} = 0.89$ mm and uniformity coefficient $C_u = 1.52$; specific gravity of that sand was 2.65, extremal void ratios were 0.56 and 0.89, and the initial void ratio of prepared samples was $e = 0.66$. Steel and polyamide were used as the fiber material. Polyamide is not a material likely to be used as a permanent soil reinforcement (because of deterioration of mechanical properties and moisture sensitivity), but its availability in a variety of sizes, and mechanical behavior common to other synthetics, makes it a convenient material to use in tests.

Triaxial drained tests on specimens of fiber-reinforced soil were performed. The height of specimens was 9.65 cm (3.8 in.) with the diameter-to-height ratio equal to one. This ratio is larger than that for a typical triaxial specimen; it was purposely selected equal to one to avoid strain localization during tests. Strain localization introduces significant difficulties in interpreting recorded displacements in terms of fiber strains. No strain localization was noticed during the tests performed. The boundary friction effects were minimized by using double layers of silicon grease-lubricated rubber membranes at both ends of the specimens.

Lengths of fibers were close to 2.54 cm (1 in.) in all cases, with the aspect ratio adjusted by varying the diameter of fibers. Each specimen was prepared in five premixed portions to ensure a uniform spatial distribution of fibers. When placing the soil in the mold, the fibers were clearly assuming anisotropic orientation with the horizontal being the preferred direction. Therefore, each part of the specimen was placed over a grid of wires and the grid was pulled through the prepared material, altering the orientation of a portion of the fibers; this led to a nearly isotropic distribution of fiber orientation (the wires in the grid were spread every 3 cm or 1.2 in.). Reinforced and unreinforced specimens were prepared in the same fashion. The nearly uniform distribution of fiber orientation was found by visual inspection, when some specimens were disassembled layer by layer and the fibers were gradually exposed (the matrix was held together by apparent cohesion).

Figure 3 shows the stress-strain behavior of the composite specimens during drained triaxial tests at a confining pressure of 400 kPa. As expected, the limit stress (or the stress at the peak) is larger for a larger aspect ratio, the fiber content being comparable. The stiffness, however, drops considerably when the aspect ratio η of polyamide fibers is increased from 85 to 180, volumetric concentration being 0.5 percent. The internal friction angle of the granular soil at this confining stress was measured to be 37.1 degrees, and the fiber-matrix interface friction angle was 20 and 14 degrees for the steel and polyamide, respectively. The yield point for both materials is roughly 0.7 and 200 MPa; it was not reached in fibers during the tests. Angle φ_w was measured in a test where the monofilament fiber was pulled out from the soil mass placed in a box and also in a direct shear test in which the matrix soil was dragged over a sheet of fiber material. The second test is preferred because the former has inherent uncertainties in interpretation of the stress state in the soil surrounding the fiber.

Figure 3 indicates that, even though the polyamide surface friction angle is less than that for steel, the deviatoric stress at failure for the composite reinforced with polyamide is greater than that reinforced with steel (for a comparable case of $\rho = 0.5$ percent and $\eta = 85$). This demonstrates that the stress induced in the polyamide is larger than that in steel fibers. Polyamide fibers probably did not assume perfectly straight shape after specimen preparation, giving rise to a stress transfer mechanism other than simple friction. Some irreversible flexural deformation was observed on disassembling the specimens, and it was noticed that polyamide fibers also experienced some local damage (but not rupture failure). It was then concluded that it is not the tensile strength of the fibers but the load transfer mechanism that has a detrimental effect on the behavior of the composite.

A comparison of the experimentally derived failure criterion and its theoretical prediction based on the limit analysis homogenization scheme presented in the previous section is shown in Figure 4. This comparison is shown for steel fibers only. It was found in experiments that the polyamide fibers did not retain their straight (linear) shape during tests, but the fibers were assumed to be straight cylinders in the modeling effort. Refinement of the model, including the influence of the fiber flexibility, is yet to be attempted.

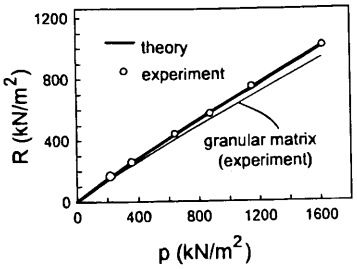

FIGURE 4 Maximum shear stress envelopes for steel fiber-reinforced sand (slip mode of failure).

In the stress range in Figure 4 the fibers did not yield, and the entire energy dissipation occurred from fiber slip in the deforming matrix. The failure condition is nonlinear, however, as a result of accounting for the variation of the matrix internal friction angle with stress (in the range indicated: 43 to 35.9 degrees). Although steel fibers are not a very effective reinforcement, Figure 4 reveals an exceptionally small discrepancy between the experimental and the theoretical results.

EXAMPLE OF APPLICATION

The limit load on a reinforced slope on a firm foundation was calculated using the slip-line method. Two cases are considered: one with fiber reinforcement and a second one with a "traditional" reinforcement (a geogrid, for instance). In both cases the material is homogenized, and the amount of reinforcement is characterized by $\rho\sigma_0$, where ρ is the volumetric fraction of the reinforcement fibers, and σ_0 is the yield stress of the reinforcing material. In the case of unidirectional reinforcement, the macroscopic continuum is, of course, anisotropic (*12*).

The slip-line fields for a slope of inclination angle of 55 degrees and soil internal friction angle of 40 degrees are shown in Figure 5. The aspect ratio of the fibers is 150, interfacial friction angle $\varphi_w = 25$ degrees, and the slope is characterized by dimensionless parameter $\gamma H/\rho\sigma_0 = 0.32$ (γ = unit weight of soil, H = slope height). The average limit load was calculated, and it is given in dimensionless fashion: for a fiber-reinforced slope $\bar{q}/\rho\sigma_0 = 2.77$, and for horizontal ("traditional") reinforcement $\bar{q}/\rho\sigma_0 = 10.89$. Such outcome is not surprising because all the reinforcement placed in the horizontal direction is used in tension. Fibers are not all effectively used.

FINAL REMARKS

Potential applications of fiber reinforcement are in infrastructure for transportation, such as subgrades for roads and airfields, embankment slopes, and so forth. Stability analyses of such structures require that the failure criterion for the fiber composite be known. An effort toward describing the stress state at failure of a fibrous granular composite was presented. An energy-based homogenization technique was shown to be a good tool to average the stresses in the composite.

The failure condition was found in the form of two functions, one related to tensile failure of fibers and the other associated with fiber slip. The first represents the shear strength as a nonlinear function of mean stress, whereas the second is linear (unless the variability of the internal friction angle with stress is taken into account). The transition from one failure mode to another is smooth. Neither theoretical nor laboratory test results indicate that the failure condition consists of two piecewise linear segments, as is often suggested.

The failure criterion derived is applicable to fiber-reinforced granular composites where the straight cylinder shape of fibers is preserved during deformation process (such as the steel fiber–reinforced sand tested here). Including the fiber flexibility in the model, with all its consequences to fiber-matrix interaction, is yet to be attempted.

The parameters needed to predict the strength of the fiber-reinforced soil are the soil internal friction angle (φ), volumetric content of fibers (ρ), fiber-soil interface friction angle (φ_w), fiber aspect ratio (η), and the yield point of the fiber material (σ_0). They all have a very clear interpretation.

The failure criterion derived can be used in limit analyses of geotechnical structures, or it can be used in finite element calculations as part of the constitutive model for the composite. Refinement of the theoretical description needs to be directed toward capturing more realistic mechanisms of fiber-matrix interaction.

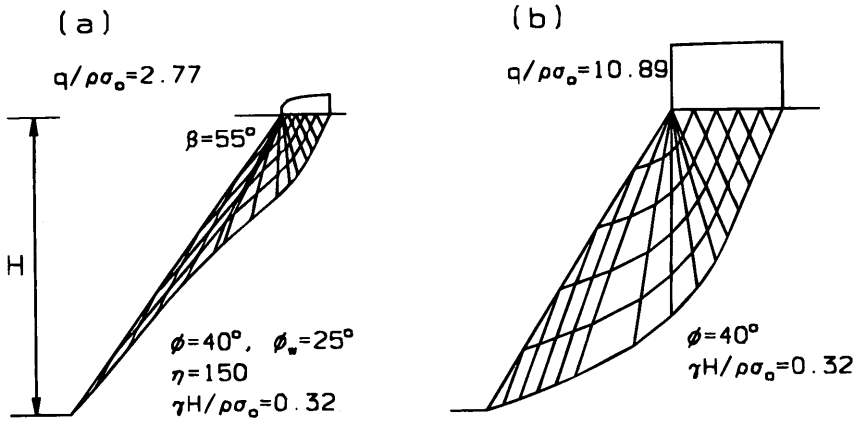

FIGURE 5 Slip-line fields for slope limit load calculations: (a) fiber reinforcement; (b) unidirectional (horizontal) reinforcement.

ACKNOWLEDGMENTS

The work presented in this paper was sponsored by the Air Force Office of Scientific Research, grant No. F49620-93-1-0192, and by the National Science Foundation, under grant No. MSS-9301494. This support is gratefully acknowledged.

REFERENCES

1. Leflaive, E., and Ph. Liausu. The Reinforcement of Soils by Continuous Threads. *Proc., 3rd International Conference on Geotextiles,* Vienna, Austria, Vol. 4, 1986, pp. 1159–1162.
2. Hill, R. A Self-Consistent Mechanics of Composite Materials. *Journal of the Mechanics and Physics of Solids,* Vol. 13, 1965, pp. 213–222.
3. Budiansky, B. On the Elastic Moduli of Some Heterogeneous Materials. *Journal of the Mechanics and Physics of Solids,* Vol. 13, 1965, pp. 223–227.
4. Mori, T., and K. Tanaka. Average Stress in Matrix and Average Elastic Energy of Materials With Misfitting Inclusions. *Acta Metallurgica,* Vol. 21, 1973, pp. 571–574.
5. Dvorak, G. J., M. S. M. Rao, and J. Q. Tarn. Generalized Initial Yield Surfaces for Unidirectional Composites. *Journal of Applied Mechanics,* ASME, Vol. 41, 1974, pp. 249–253.
6. Hashin, Z. Analysis of Composite Materials: A Survey. *Journal of Applied Mechanics,* ASME, Vol. 50, 1983, pp. 481–505.
7. Sawicki, A. Plastic Limit Behavior of Reinforced Earth. *Journal of Geotechnical Engineering,* Vol. 109, No. 7, 1983, pp. 1000–1005.
8. de Buhan, P., R. Mangiavacchi, R. Nova, G. Pellegrini, and J. Salençon. Yield Design of Reinforced Earth Walls by Homogenization Method. *Géotechnique,* Vol. 39, No. 2, 1989, pp. 189–201.
9. de Buhan, P., and L. Siad. Influence of a Soil-Strip Interface Failure Condition on the Yield-Strength of Reinforced Earth. *Computers and Geotechnics,* Vol. 7, Nos. 1 & 2, 1989, pp. 3–18.
10. di Prisco, C., and R. Nova. A Constitutive Model for Soil Reinforced by Continuous Threads. *Geotextiles and Geomembranes,* Vol. 12, 1993, pp. 161–178.
11. Michalowski, R. L., and A. Zhao. Limit Loads on Fiber-Reinforced Earth Structures. *Proc., 13th International Conference of Soil Mechanics and Foundation Engineering,* New Delhi, India, Vol. 2, 1994, pp. 809–812.
12. Michalowski, R. L., and A. Zhao. Failure Criteria for Fibrous Granular Composites. In *Computer Methods and Advances in Geomechanics* (H. J. Siriwardane and M. M. Zaman, eds.), Vol. 2, 1994, pp. 1385–1390.
13. Andersland, O. B., and A. S. Khattak. Shear Strength of Kaolinite/Fiber Soil Mixtures. *Proc., International Conference on Soil Reinforcement: Reinforced Soil and Other Techniques,* Paris, France, Vol. 1, 1979, pp. 11–16.
14. Hoare, D. J. Laboratory Study of Granular Soils Reinforced With Randomly Oriented Discrete Fibers. *Proc., International Conference on Soil Reinforcement: Reinforced Soil and Other Techniques,* Paris, France, Vol. 1, 1979, pp. 47–52.
15. Arenicz, R. M., and R. N. Chowdhury. Laboratory Investigation of Earth Walls Simultaneously Reinforced by Strips and Random Reinforcement. *Geotechnical Testing Journal,* Vol. 11, 1988, pp. 241–247.
16. Gray, D. H., and H. Ohashi. Mechanics of Fiber Reinforcement in Sand. *Journal of Geotechnical Engineering,* Vol. 109, 1983, pp. 335–353.
17. Maher, M. H., and D. H. Gray. Static Response of Sands Reinforced With Randomly Distributed Fibers. *Journal of Geotechnical Engineering,* Vol. 116, 1990, pp. 1661–1677.
18. Hashin, Z. Transverse Strength, In *Evaluation of Filament Reinforced Composites for Aerospace Structural Applications,* NASA CR-207, (N. F. Dow and B. W. Rosen, eds.), 1964, pp. 36–43.
19. Shu, L. S., and B. W. Rosen. Strength of Fiber-Reinforced Composites by Limit Analysis Methods. *Journal of Composite Materials,* Vol. 1, 1967, pp. 366–381.
20. McLaughlin, P. V., and S. C. Batterman. Limit Behavior of Fibrous Materials. *International Journal of Solids and Structures,* Vol. 6, 1970, pp. 1357–1376.
21. Davis, E. H. Theories of Plasticity and the Failure of Soil Masses. In *Soil Mechanics: Selected Topics* (I. K. Lee, ed.), Butterworth, London, England, 1968, pp. 341–380.
22. Drescher, A., and E. Detournay. Limit Load in Translational Failure Mechanisms for Associative and Non-Associative Materials. *Géotechnique,* Vol. 43, No. 3, 1993, pp. 443–456.

Publication of this paper sponsored by Committee on Soil and Rock Properties.